The implementation of concave micro optical devices using a polymer dispensing technique

Sheng-Yi Hsiao[1], Chih-Chun Lee[1] and Weileun Fang[1,2]

[1] Power Mechanical Engineering, National Tsing Hua University, Hsinchu 30013, Taiwan
[2] NEMS Institute, National Tsing Hua University, Hsinchu 30013, Taiwan

E-mail: fang@pme.nthu.edu.tw

Abstract
This study demonstrates a novel approach to implementing a double-concave (DCV) microlens using a simple polymer dispensing and sucking process. The DCV microlens is implemented at room temperature using a commercially-available pneumatic-controlled polymer dispensing system. The DCV lens profile can be tuned by varying the volume of the dispensed polymer. It is also easy to integrate the present polymer DCV microlens with other suspended micromachined devices such as silicon nitride film and silicon-on-glass (SOG) micromachined structures. This study further employs the process for DCV to implement a concave mirror. The measurement results show a typical DCV lens (made of NOA63 polymer) with negative focal lengths of −1.42 mm (red laser) and −1.17 mm (blue laser), and a concave mirror with a focal length of 3.28 mm. Moreover, this study also demonstrates the integration of a DCV microlens with other optical components, such as plano-convex and double-convex lenses.

(Some figures in this article are in colour only in the electronic version)

1. Introduction

A microlens is a key component in microoptoelectromechanical systems (MOEMS) and has applications in various fields. Plano-convex (PCX) and double-convex (DCX) polymer microlenses are extensively reported using dispensing and reflowing approaches [1–4]. The applications of these components include fiber connectors, light sources collimation [5, 6], pixel-based electronic imaging [7], confocal microscopy [8] and direct optical imaging [9]. The active tuning of a lens shape is also demonstrated using various approaches, including electro wetting tunable lenses [10–12], liquid-filled tunable lenses [13–15], thermal actuated solid tunable lenses [16, 17] and a liquid crystal immersed approach [18]. The integration of concave and convex microlenses creates additional applications such as correcting spherical and chromatic aberration. A concave mirror surface prepared using a selective polishing method is reported in [19]. Plano-concave (PCV) lenses achieved using different methods are also reported. For instance, the plano-concave lens array is presented using inverse replication molding from a convex lens array [20]. Moreover, other techniques such as gray-tone mask [21], excimer laser [22] and gray-scale oxidation [23] are employed to fabricate a micro lens of arbitrary shape. However, the fabrication process and the following device integration of these techniques are not straightforward.

Double-concave (DCV) micro optical components, on the other hand, are rarely investigated. In this study we propose a convenient, simple polymer dispensing and sucking process to implement double-concave (DCV) microlenses. An approach to predict and implement the lens shape of DCX formed by the liquid-phase UV-curable polymer has been reported in [1]. The lens shape of concave-based optical components formed by a liquid polymer can also be predicted using a similar approach. This research further presents the design of a novel DCV micro optical lens component by dispensing and curing a liquid-phase polymer material. The DCV lens is realized on a micromachined lens frame by a polymer dispensing and sucking processes. A schematic of a DCV lens and its frame
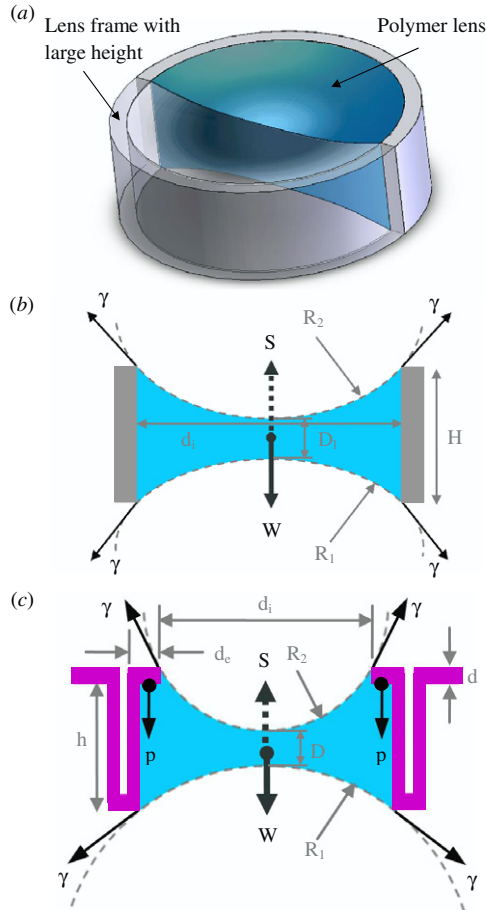
Figure 1. (*a*) Schematic diagram of the polymer lens on a hollow cylinder frame, (*b*) the dimensions of the lens and frame, and the forces applying on the liquid polymer lens and (*c*) the polymer lens on a different frame structure design.

is illustrated in figure 1. The lens profiles can be tuned by varying the volume of the dispensed polymer. The optical performance of the DCV lens is characterized by capturing focused laser beam images. The experimental results reveal the feasibility of the dispensed DCV microlens. In addition, the concepts of the concave-mirror and the doublet are also realized by adding some simple steps after the fabrication of the DCV lens.

2. Concepts and design

The design concept of this study is schematically illustrated in figure 1(*a*). The liquid phase polymer forms a DCV shape after being trapped inside a hollow cylinder frame of large height H. Thus, a DCV lens is implemented after the solidification of the polymer. The frame height H provides the space to contain the lens sags on both upper and lower sides. As shown in figure 1(*b*), the edge thickness and size of the DCV lens are determined by the frame height H and inner diameter d_i of the hollow cylinder, respectively. The liquid polymer on the hollow cylinder is assumed to have spherical surface profiles with curvatures of R_1 and R_2. Thus, the volume V of the liquid polymer can be extracted from the parameters of H, d_i, R_1

and R_2:

$$V = \frac{\pi}{4}Hd_i^2 - \frac{\pi}{3}\left(2R_2^3 + 2R_1^3\right)$$

$$+ \frac{\pi}{3}\left[2R_2^2 + \left(\frac{d_i}{2}\right)^2\right]\left[R_2^2 - \left(\frac{d_i}{2}\right)^2\right]^{\frac{1}{2}}$$

$$+ \frac{\pi}{3}\left[2R_1^2 + \left(\frac{d_i}{2}\right)^2\right]\left[R_1^2 - \left(\frac{d_i}{2}\right)^2\right]^{\frac{1}{2}}. \quad (1)$$

The liquid polymer is under the surface tension force S and gravity force W. Assuming that the polymer material has a density of ρ and a surface tension of γ, the equation to meet the static equilibrium condition, $S = W$, is expressed as

$$S(\gamma, R_1, R_2, d_i) = \rho G \times V(R_1, R_2, H, d_i) \quad (2)$$

where G is the gravity, and the net surface tension force term can be expressed as

$$S = \frac{1}{2}\pi\gamma \times d_i^2 \times \left(\frac{1}{R_2} - \frac{1}{R_1}\right). \quad (3)$$

In this study, the frame dimensions H and d_i, and the material properties ρ and γ of the polymer are the prescribed design parameters. Based on equations (1)–(3), the lens curvatures R_1 and R_2 are determined by a given polymer volume V. The shape of a liquid polymer trapped inside a more complicated frame structure can also be predicted in the same manner. For instance, figure 1(*c*) shows a frame structure made of a thin film material with thickness d. To provide sufficient space for DCV lens, the supporting frame also has a large height h. Two additional geometry parameters, including the inner diameter d_i and the edge width d_e of the frame depicted in the figure, are available in this design, and thus equation (1) can be rewritten as

$$V = \frac{\pi}{4}h \times (d_i + 2d_e - 2d)^2 + \frac{\pi}{4}d \times d_i^2 - \frac{\pi}{3}\left(2R_2^3 + 2R_1^3\right)$$

$$+ \frac{\pi}{3}\left[2R_2^2 + \left(\frac{d_i}{2}\right)^2\right]\left[R_2^2 - \left(\frac{d_i}{2}\right)^2\right]^{\frac{1}{2}}$$

$$+ \frac{\pi}{3}\left[2R_1^2 + \left(\frac{d_i}{2} + d_e - d\right)^2\right]\left[R_1^2 - \left(\frac{d_i}{2} + d_e - d\right)^2\right]^{\frac{1}{2}}. \quad (4)$$

Meanwhile, the surface tension force S can also be rewritten as

$$S = \pi\gamma \times d_i^2 \times \frac{1}{2R_2} - \pi\gamma \times (d_i + 2d_e - 2d)^2 \times \frac{1}{2R_1}. \quad (5)$$

Moreover, as d_e is included in the design structure, a liquid pressure p $(=\rho Gd)$ is also acting on the lens, as shown in figure 1(*c*). The net pressure force P can be expressed as

$$P = \rho Gd \times \pi\left[\left(\frac{d_i}{2} + d_e - d\right)^2 - \left(\frac{d_i}{2}\right)^2\right]. \quad (6)$$

Consequently, the static equilibrium equation for the lens frame shown in figure 1(*c*) is yielded as

$$S(\gamma, R_1, R_2, d_i, d_e, d) = \rho G \times V(R_1, R_2, h, d_i, d_e, d)$$
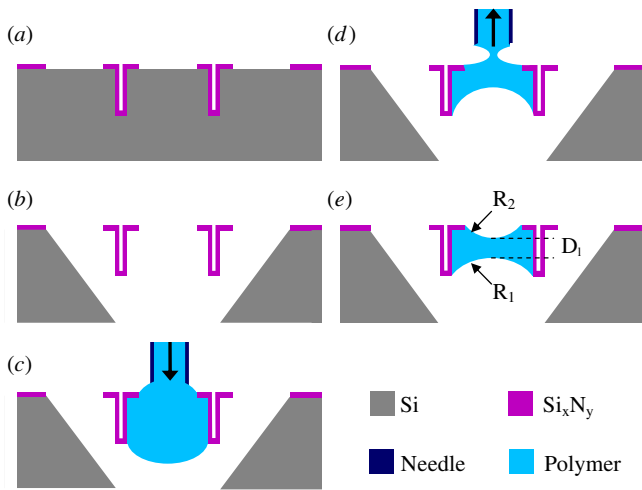$$+ P(\rho, d_i, d_e, d). \quad (7)$$

Figure 2. Process steps to fabricate the proposed DCV lens on a thin film supporting frame with large frame height *h*.

The pressure force of the micro scale polymer lens discussed in this study is roughly three orders of magnitude smaller than the gravity force, and the gravity force is three orders of magnitude smaller than the surface tension force. For instance, assume a lens geometry of 500 μm in diameter, 100 μm in height and polymer of $\rho = 1$ g cm^{-3}, $\gamma = 70$ mN m^{-1}, the gravity determined from ρGV (V as in equation (4)) is about 1.5×10^{-4} mN. In addition, the surface tension force on one curvature and the pressure determined respectively from part in equation (5) and from equation (6) are about 1.0×10^{-1} mN and 0.8×10^{-7} mN. Thus, the gravity and pressure forces in equations (2) and (7) can be ignored. In this study, the geometry parameters of the lens frame, such as h, d_e, d_i and d are specified before the dispensing of the liquid phase polymer. Thus, according to equations (1), (3)–(5), the curvatures R_1 and R_2 of the DCV lens are tuned by varying the polymer volume V during the polymer-dispensing process. On the other hand, the geometry parameters of the lens frame can also be employed to tune the polymer lens shape for a given polymer volume V. An optical characteristic, such as the focal length f of the present DCV lens, is thus determined as

$$f = \frac{1}{(n-1)\left[\frac{1}{R_1} - \frac{1}{R_2} + \frac{D_l}{R_1 R_2}\frac{n-1}{n}\right]} \qquad (8)$$

where n and D_l are the refractive index and center thickness of the polymer lens in figure 1, respectively.

3. Fabrication and results

In application, the fabrication processes in figure 2 have been established to realize the DCV lens. In addition, the realization of other optical components such as a concave mirror and the integration of various optical components such as a lens doublet can also be achieved after adding some additional processes to figure 2, as described in section 3.2.

3.1. Fabrication of the DCV lens

Figure 2 shows the process steps to implement the present DCV lens. As shown in figure 2(*a*), a deep reactive ion etch

(DRIE) is employed to etch a ring trench of depth h in a silicon substrate so as to define the height of the lens supporting frame. After that, conformal coverage of the trench with LPCVD (low pressure chemical vapor deposition) silicon-rich nitride film Si_xN_y is performed. The silicon-rich nitride film is defined by the RIE etching process to form the thin-film lens supporting frame. By means of the trench deposition process, the large frame height h is achieved. As illustrated in figure 2(*b*), the patterned lens supporting frame is released anisotropically by potassium hydroxide (KOH) silicon wet etching. The volume of polymer is then controlled by a commercial pneumatic dispensing system (Ultra 2400 dispensing workstation, EFD Inc.) to define the lens profile. As shown in figure 2(*c*), the polymer is dispensed to wet the vertical sidewall of the lens frame first. In this step, the dispensed polymer exceeds the total volume for the lens. The total polymer volume for the lens is controlled by the sucking back process, as shown in figure 2(*d*). After the polymer is cured in UV light, the surface profile of the polymer DCV (or DCX) lens is determined, as shown in figure 2(*e*). The dispensing of the polymer microlens is a room temperature process, and is easily integrated with other released MEMS frame structures. Another supporting frame of large frame height h, such as SOI and LIGA structures, can also be employed to implement the present concave-based polymer lens.

Figure 3(*a*) shows a scanning electron microscope (SEM) micrograph of a typical thin film lens frame and its four suspensions before polymer dispensing. The SEM micrograph in figure 3(*b*) shows the concave surface of a typical dispensed lens. Figure 3(*c*) shows an optical microscope (OM) photo of a DCV lens made of NOA63 UV-curable polymer. The transparency of the DCV lens is clearly observed in this photograph. Moreover, the concave-based polymer lens implemented on a bulk silicon hollow cylinder frame is also demonstrated, as shown in figures 3(*d*) and (*e*). The lens frame is made of the single crystal silicon device layer on a SOG wafer using DRIE etching.

3.2. Other available optical components

This research further integrates the fabrication steps in figure 2 with additional processes to demonstrate other concave-based micro optical components, and integrates the DCV lens with other optical components as well. As illustrated in figure 4(*a*), a concave mirror can be realized after having deposited a reflective metal film onto the polymer DCV lens. The photo in figure 4(*b*) demonstrates a typical concave mirror fabricated after depositing an Al film on the DCV lens shown in figure 3(*c*). As shown in this photo, the mirror reflects the light and image on the inspecting side. As illustrated in figure 4(*c*), a lens doublet can be achieved after sequential dispensing another polymer material (polymer 2 in figure 4(*c*)) of different material property onto the DCV lens. The photo in figure 4(*d*) demonstrates the integration of a doublet made of AZ4620 photo-resist (DCV lens) and NOA63 (DCX lens). Since the NOA63 DCX lens is transparent, the color of the AZ4620 DCV lens underneath is easily observed.

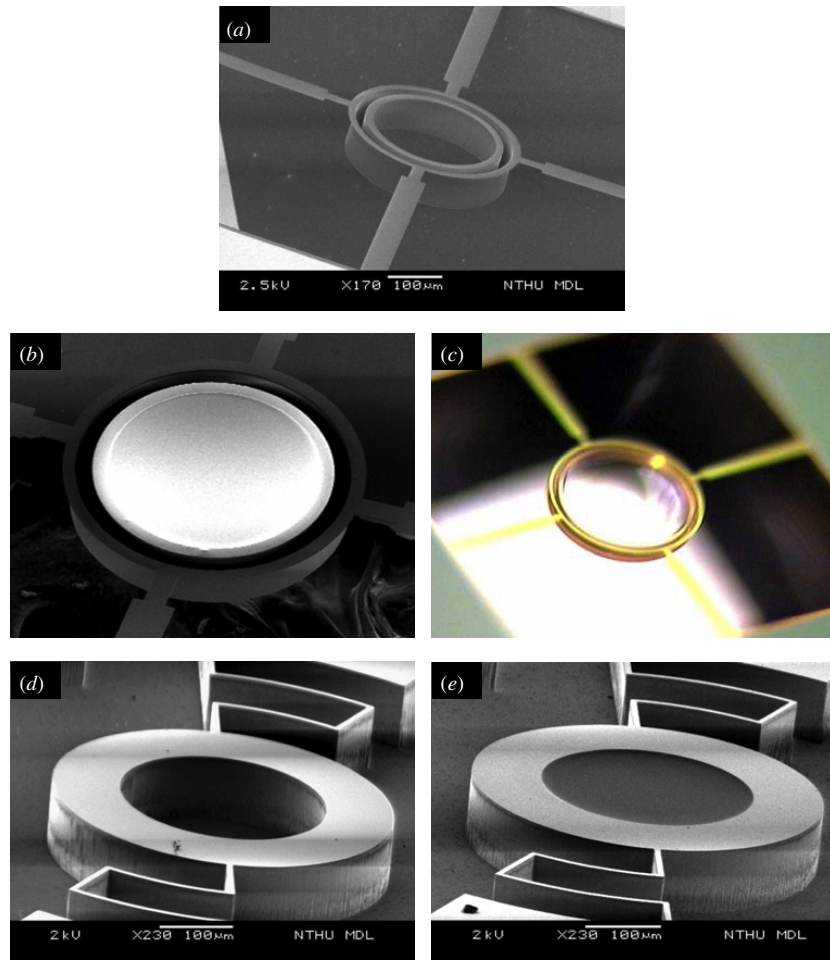Moreover, the concept of integrating a polymer DCV lens with a PCX glass lens is illustrated in figure 5(*a*).

Figure 3. Typical fabrication results. SEM micrographs of a thin film supporting frame (*a*) before and (*b*) after the formation of a polymer DCV lens. (*c*) OM images of a DCV lens. SEM micrographs of a SOG lens supporting frame (*d*) before and (*e*) after the forming of a DCV lens.
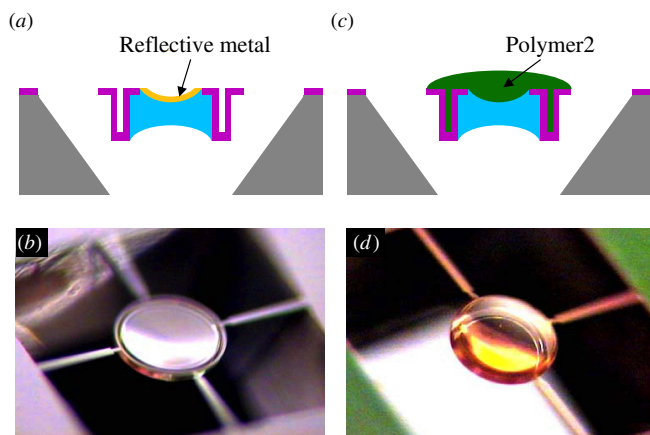

Figure 4. (*a*) Schematic of a concave mirror fabricated from a polymer DCV lens; (*b*) OM photo of a typical fabricated concave mirror. (*c*) Schematic of the DCV/DCX doublet component integration; (*d*) OM photo of a typical fabricated doublet formed by PR-DCV and NOA63-DCX.

After defining the thin-film lens supporting frame shown in figure 2(*a*), the silicon substrate is experiencing a backside DRIE to form a cavity. The wafer is then bonded to a pyrex 7740 glass in a vacuum. As shown in figure 5(*a*), a glass reflow process (GFP) [24] is employed to form a convex glass lens. In this process, a high temperature is required to allow the reflow of pyrex 7740 glass, and the reflow of the pyrex 7740 glass is driven by the pressure difference between the ambient and the vacuum cavity. The glass of the mirror flat surface is achieved after the lapping and CMP (chemical mechanical polishing) processes. After that, wet etching and dispensing processes, as illustrated in figures 2(*b*)–(*e*), are used to fabricate the polymer DCV lens. The typical integration of a GFP lens and polymer lens is demonstrated in figure 5(*b*). As a result, the integration of concave-based lenses with other optical components can also be realized in a similar manner.

4. Lens characterization and testing

The performance of the fabricated DCV lens has been characterized to demonstrate the feasibility of the present concept. In order to confirm the formation of the DCV lens, its surface profiles R_1 and R_2 are measured using an optical interferometer. Figure 6 shows the typical measurement results for the lens illustrated in figure 1(*c*). The measured lens curvatures R_1 and R_2 are 21.47 mm and 21.39 mm, respectively.
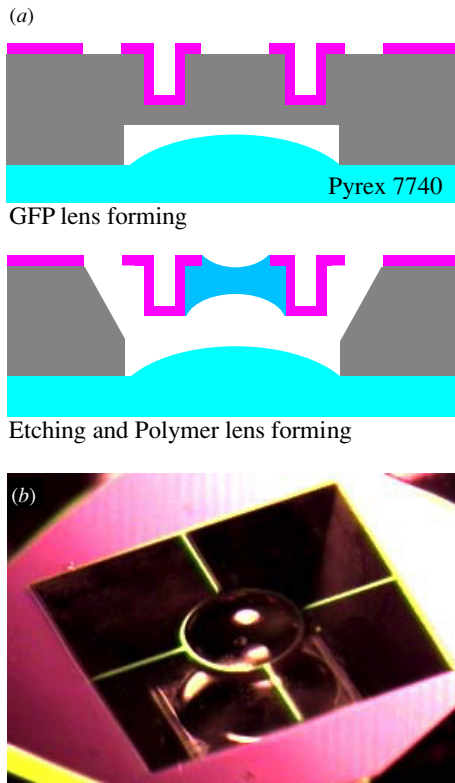
(*a*)

GFP lens forming

Etching and Polymer lens forming

(*b*)

Figure 5. (*a*) Schematic of the GFP and polymer lens integration processes and (*b*) OM photo of typical fabricated lens integration.
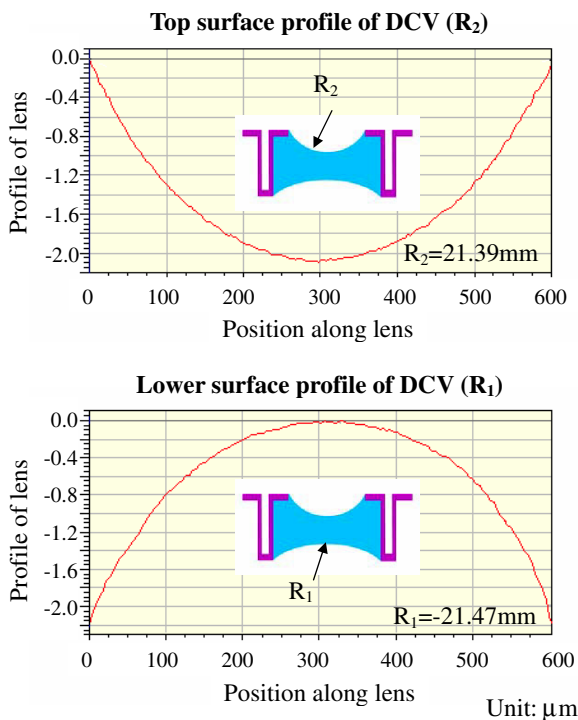
Top surface profile of DCV (R₂)

R_2

$R_2=21.39\text{mm}$

Position along lens

Lower surface profile of DCV (R₁)

R_1

$R_1=-21.47\text{mm}$

Position along lens

Unit: μm

Figure 6. The typical double side surface profiles of a DCV lens measured by an optical interferometer.

In this case, the inner diameter is $d_i = 1000$ μm, the edge width is $d_e = 15$ μm, the film thickness is $d = 0.5$ μm, the thick of the lens is $h = 80$ μm and the center 600 μm diameter profiles

Lens shape vs. Polymer volume

- ● - Measured (R₁)
- ✕ - Measured (R₂)
- ▲ Analysis (R₁)
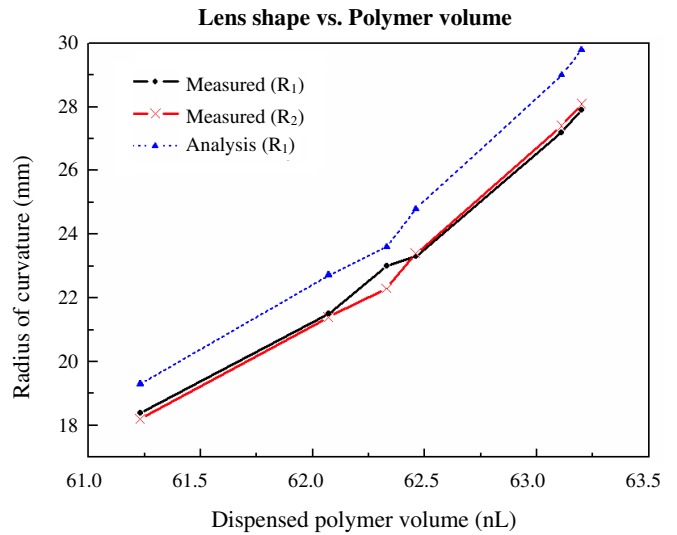
Figure 7. Analysis and measurements of lens curvatures for different volumes of the dispensing polymer.

R₂ profile of DCV   **R₂ profile of DCX**

$R_2=1.14\text{mm}$ $R_2=-0.81\text{mm}$

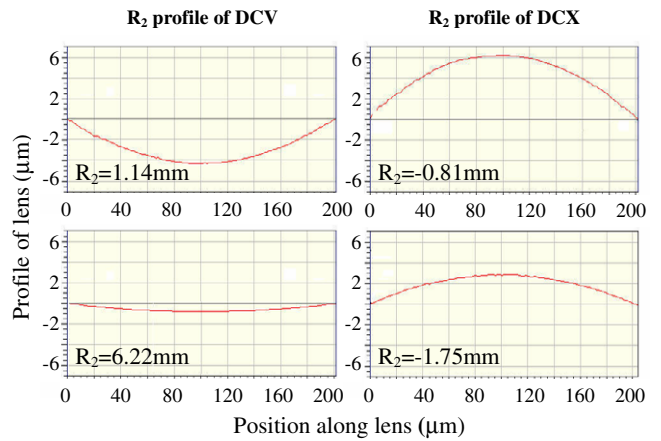$R_2=6.22\text{mm}$ $R_2=-1.75\text{mm}$

Position along lens (μm)

Figure 8. The DCX and DCV lens surface profile R_2 tuned by varying the volume of the dispensed polymer.

are measured. The applied NOA63 on silicon nitride film is tested in air with a surface tension of 68 mN m⁻¹. The gravity and pressure forces in equation (7) are inconsequential to this study; and the lens profiles are predicted with equation (5). As a result, the predicted lens curvatures of R_1 and R_2 are within 5.9% difference based on equation (5). Thus, the experimental results agree well with the prediction from equation (5).

Figure 7 shows six measurements of lens curvatures for different volumes of the dispensing polymer. The results demonstrate the variation of the lens curvature with the polymer volume. The results also agree with the prediction that R_1 will be close to R_2 from equation (5). As a comparison, the radii of curvatures R_2 are predicted from equation (5), and the deviation between the analysis and experiment ranges from 2.6% to 6.3%. Moreover, the lens profile can also be changed from DCX to DCV by the dispensing and sucking processes in figures 2(*c*) and (*d*). Figure 8 demonstrates four 300 μm diameter polymer micro lenses of different lens profiles. The center 200 μm diameter measurement results show the
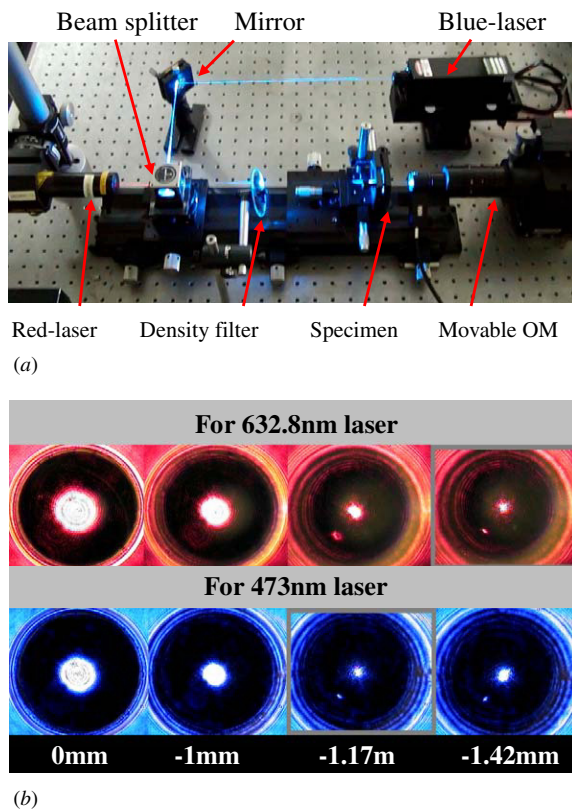
Figure 9. (*a*) Experimental setup for the lens test and (*b*) virtual images captured by OM focusing at different positions. The position '0 mm' indicates the focal plane of OM located at the substrate surface. The negative sign represents virtual images captured at the R_1 side.

variation of the surface profile R_2 for DCV and DCX lenses. Figure 9(*a*) shows the experimental setup used to record virtual focal images of the DCV lens. In this experiment, both a 632.8 nm He–Ne laser and a 473 nm diode laser are used. Two laser beams are aligned on the same axis and incident into the lens, and the focused images are captured by a movable CCD. Figure 9(*b*) shows typical measurement results for a 500 μm diameter DCV lens where $R_1 = -1.64$ mm, $R_2 = 1.61$ mm and the lens thickness $D_l = 0.031$ mm. The measured focal length is -1.42 mm for the 632.8 nm red laser, and -1.17 mm for the 473 nm blue laser. In addition, the measured focal length of a concave mirror with radius of curvature $R = 6.39$ mm is 3.28 mm. The measurement agrees with the result predicted from $R/2$.

5. Conclusions

This study demonstrates a DCV microlens using a liquid polymer forming process. In general, a DCV lens can be implemented by a simple polymer dispensing and sucking process on a MEMS supporting structure of sufficient height. The lens profile can be tuned from DCV to DCX by varying the volume of the dispensed polymer. In application, the DCV polymer lens has been successfully realized on silicon nitride film and SOG MEMS structures. The focused laser beam images of a typical fabricated DCV lens were characterized for both a red laser and a blue laser. The measurements show the feasibility of the lens forming and the optical function. Further implementation of various optical components such as concave mirrors, doublets and lens integration is also demonstrated.

References

[1] Hsieh J, Hsiao S-Y, Lai C-F and Fang W 2007 Integration of a UV curable polymer lens and MUMPs structures on a SOI optical bench *J. Micromech. Microeng.* **17** 1703–9
[2] Kwon S, Milanovic V and Lee L P 2002 Large-displacement vertical microlens scanner with low driving voltage *IEEE Photon. Technol. Lett.* **14** 1572–4
[3] Toshiyoshi H, Su G-D J, LaCosse J and Wu M C 2003 A surface micromachined optical scanner array using photoresist lenses fabricated by a thermal reflow process *J. Lightw. Technol.* **21** 1700–8
[4] Lin Y-S, Pan C-T, Lin K-L, Chen S-C, Yang J-J and Yang J-P 2001 Polyimide as the pedestal of batch fabricated micro-ball lens and micro-mushroom array *Proc. MEMS 2001 (Jan.)* pp 337–40
[5] Jeon C W, Gu E, Liu C, Girkin J M and Dawson M D 2005 Polymer microlens arrays applicable to AlInGaN ultraviolet micro-light-emitting diodes *IEEE Photon. Technol. Lett.* **17** 1887–9
[6] Park E-H, Kim M-J and Kwon Y-S 1999 Microlens for efficient coupling between LED and optical fiber *IEEE Photon. Technol. Lett.* **11** 439–41
[7] Fan Y-T, Peng C-S and Chu C-Y 2000 Advanced microlens and color filter process technology for the high-efficiency CMOS and CCD image sensors *Proc. SPIE* **4115** 263–74
[8] Jain A and Xie H 2007 Microendoscopic confocal imaging probe based on an LVD microlens scanner *IEEE J. Sel. Top. Quantum Electron.* **13** 228–34
[9] Tohara M, Iwase E, Hoshino K, Matsumoto K and Shimoyama I 2005 Pop-up display with 3-dimensional microlens structures *Proc. MEMS 2005 (Feb. 2005)* pp 231–4
[10] Krupenkin T, Yang S and Mach P 2003 Tunable liquid microlens *Appl. Phys. Lett.* **82** 316–8
[11] Hsieh W H and Chen J H 2005 Lens-profile control by electrowetting fabrication technique *IEEE Photon. Technol. Lett.* **17** 606–8
[12] Kuiper S and Hendriks B H W 2004 Variable-focus liquid lens for miniature cameras *Appl. Phys. Lett.* **85** 1128–30
[13] Chtonis N, Liu G L, Jeong K H and Lee L P 2003 Tunable liquid-filled microlens array integrated with microfluidic network *Opt. Express* **11** 2370–8
[14] Sugiura N and Morita S 1993 Variable-focus liquid-filled optical lens *Appl. Opt.* **32** 4181–5

[15] Zhang D Y, Justis N and Lo Y H 2004 Fluidic zoom-lens-on-a-chip with wide field of view tuning range *IEEE Photon. Technol. Lett.* **16** 2356–8

[16] Lee S Y, Tung H W, Chen W C and Fang W 2006 Thermal actuated solid tunable lens *IEEE Photon. Technol. Lett.* **18** 2191–3

[17] Lee S Y, Chen W C, Tung H W and Fang W 2007 Microlens with tunable astigmatism *IEEE Photon. Technol. Lett.* **19** 1383–5

[18] Fang Y H, Ren H H, Liang X, Wang H and Wu S T 2005 Liquid crystal microlens arrays with switchable positive and negative focal lengths *J. Display Technol.* **1** 151–5

[19] Kanbara N, Tezuka S-I and Watanabe T 2006 MEMS tunable VCSEL with concave mirror using the selective polishing method *Proc. IEEE Optial MEMS 2006 (Aug.)* pp 9–10

[20] Desmet L, Overmeire S V, Erps J J V, Ottevaere H, Debaes C and Thienpont H 2007 Elastomeric inverse moulding and vacuum casting process characterization for the fabrication of arrays of concave refractive microlenses *J. Micromech. Microeng.* **17** 81–8

[21] Oppliger Y, Sixt P, Stauffer J M, Mayor J M, Regnault P and Voirin G 1994 One-step 3D shaping using a gray-tone mask for optical and microelectronic applications *Microelectron. Eng.* **23** 449–54

[22] Lee Y-C, Chen C-M and Wu C-Y 2005 A new excimer laser micromachining method for axially symmetric 3D microstructures with continuous surface profiles *Sensors Actuators* A **117** 349–55

[23] Chen C-F, Tzeng S-D, Chen H-Y and Gwo S 2005 Silicon microlens structures fabricated by scanning-probe gray-scale oxidation *Opt. Lett.* **30** 652–4

[24] Merz P, Quenzer H J, Bernt H, Wagner B and Zoberbier M 2003 A novel micromachining technology for structuring borosilicate glass substrates *Proc. Transducers '03 (Boston, USA, June 8–12)* pp 258–61